Calculation of Flow Distribution in Large Radius Ratio Stages of Axial Flow Turbines and Comparison of Theory and Experiment[1]

JOSEF HERZOG

General Electric Company

This paper describes a method of calculating stage parameters and flow distribution of axial turbines. The governing equations apply to space between the blade rows and are based on the assumption of rotationally symmetrical, compressible, adiabatic flow conditions. Results are presented for stage design and flow analysis calculations. Theoretical results from the calculation system are compared with experimental data from low pressure steam turbine tests.

Modern steam turbines expand water vapor in 20 to 25 stages from a pressure of 3400 psia, 1050° F to about 0.80 psia, 94° F and handle thereby an 1800:1 increase in volume flow. Subdivision of the steam path into high pressure, intermediate pressure, and low pressure cylinders[2] makes the magnitude of pressure, temperature, and specific volume changes technically acceptable within each of the three units. The large volume flows at the low pressure end are handled by adding the appropriate number of low pressure turbines.

We will discuss one step in the steam path layout of such a low pressure turbine: the method of determining blade flow angles and calculating flow distribution in a sharply divergent, locally transonic flow field (ref. 1).

Comparison of analytical predictions with low pressure test turbine results is the second subject of this paper. The calculation method is based on the well known "streamline curvature method" assuming rotationally symmetrical flow. The resulting circumferentially averaged information is used as a basis for the profile design.

---

[1] The author gratefully acknowledges the contributions of a great number of colleagues and expresses appreciation to Mr. J. E. Fowler and to the General Electric Company for permitting this publication.

[2] A "cylinder" designates a separate housing.

DERIVATION OF WORKING EQUATIONS AND CALCULATION PROCEDURE

The equations of motion and the continuity equation are transformed from a cylindrical coordinate system into a system with the stream function and the axial distance as independent variables. The meridional streamlines, along which the stream function is a constant, are approximated by polynomials. These transformed equations and an assumed isentropic pressure density relationship in stream direction allow determination of the axial velocity derivative and the pressure gradient in a radial direction at any axinormal plane (called "station") outside a blade row. Derivation of the equations is given and one cycle of an iterative solution is discussed in this section.

The Euler equations for steady state inviscous rotationally symmetrical flow without body forces in a cylindrical coordinate system,

$$\left.\begin{aligned} uu_r+wu_z-\frac{v^2}{r}&=-\frac{1}{\rho}P_r \\ uv_r+wv_z+\frac{uv}{r}&=0 \\ uw_r+ww_z&=-\frac{1}{\rho}P_z \end{aligned}\right\} \quad (1)^3$$

and the equation of continuity

$$(\rho ur)_r+(\rho wr)_z=0 \quad (2)$$

are transformed into the ψ,z plane. P designates the static pressure and ρ the fluid density. Coordinate system and velocity components are shown in figure 1. ψ is a stream function defined by the differential expression

$$d\psi=2\pi\rho rw\cdot dr-2\pi\rho ru\cdot dz=\psi_r\cdot dr+\psi_z\cdot dz \quad (3)$$

Setting $u=w\sigma$ (σ being the streamline slope in the meridional plane) and $v=\Gamma/r$, $2\pi=k$, leads to the following set of equations in the ψ,z plane:

$$\frac{1}{kr}(\sigma w)_z-\frac{\Gamma^2}{wkr^4}=-P_\psi \quad (4)$$

$$\Gamma_z=0 \quad (5)$$

---

[3] Partial derivatives are indicated by the coordinate subscripts.

FIGURE 1.—*Coordinate system and velocity components.*

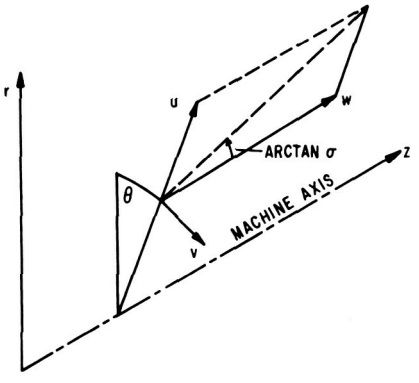

$$ww_z - kr\sigma wP_\psi = -\frac{1}{\rho}P_z \tag{6}$$

$$k\rho^2 r^2 w^2 \sigma_\psi + \rho(wr)_z + wr\rho_z = 0 \tag{7}$$

Equations (4), (5), and (6) combined yield the Bernoulli equation in differential form along a streamline

$$\left[\frac{1}{2}\left(\frac{\Gamma}{r}\right)^2 + \frac{w^2}{2}(1+\sigma^2)\right]_z + \frac{1}{\rho}P_z = 0 \tag{8}$$

Equation (4) is used for the calculation of the radial pressure distribution by iteration. In order to do this, w_z is determined from equation (7) and equation (8), assuming isentropic expansion along a streamline and known streamline shape.

$$w_z = \frac{1}{\left[1 - \dfrac{w^2\rho(1+\sigma^2)}{\gamma P}\right]}\left[\frac{w^2\rho\sigma}{\gamma P}\left(w\sigma_z - \frac{\Gamma^2}{wr^3}\right) - k\rho r w^2 \sigma_\psi - \frac{w\sigma}{r}\right] \tag{9}$$

Equations (4) and (9), applying to the fluid motion at any axial station i, (fig. 2), are supplemented by the energy equation that is valid along any streamline (ψ_j = constant) and links up thermodynamically with station $i-1$.

$$W_i^2 = (K1)W_{i-1}^2 + (K2)\frac{2\gamma_{i-1}P_{i-1}}{(\gamma_{i-1}-1)\rho_{i-1}}\left[1 - \left(\frac{P_i}{P_{i-1}}\right)^{(\gamma_{i-1}-1)/\gamma_{i-1}}\right] + \omega_i^2(r_i^2 - r_{i-1}^2) \tag{10}$$

W is the total velocity relative to the blade row at which exit station i is located. $K1$ and $K2$ are the carryover and reaction coefficients, denoting fraction of upstream kinetic energy and reaction energy accounting for

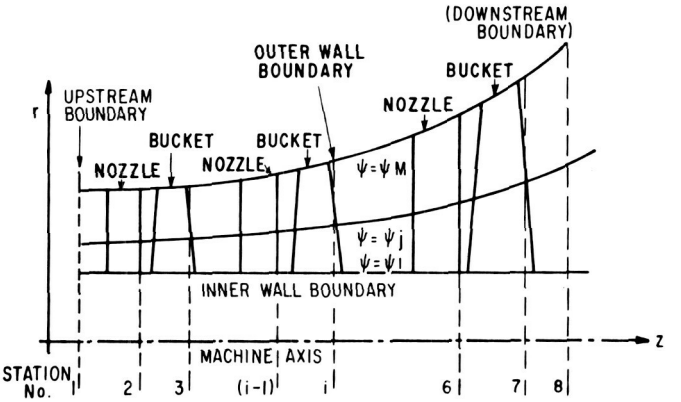

FIGURE 2.—*Grid for setup of calculation.*

the kinetic energy at station i, respectively. ω is the wheel speed and γ the specific heat ratio of the medium.

The shape of the streamlines σ and σ_z is approximated by piecewise polynomial curve fit such that

$$\sigma = AR + B \tag{11}$$

$$\sigma_z = CR + D \tag{12}$$

The coefficients of matrices A and C are functions of spacing of stations. Those of matrices B and D are functions of spacing and streamline slopes at upstream and downstream boundaries. R is the radius matrix. Only one matrix inversion is necessary at the beginning of iterations. σ_ψ is found by numerical differentiation.

Equations (4), (9), (10), (11), and (12), equation of state or steam tables, and relations for velocity triangles are the basic equations used in the iteration at a station. This system can be solved either in a design mode or in an analysis mode for each station.

The interchangability of modes permits steam path design to proceed through both new and available cascade components, besides the usual routine layout of all new stages or the analysis of an existing turbine at arbitrary flow conditions.

The sequence of calculations for a design iteration is sketched in the following:

Assume station i is to be iterated. Having just passed station $i-1$, gas conditions, velocities, and streamline shape are known as functions of ψ_j and z_{i-1}. Slopes σ_{ij} and their derivatives σ_{zij}, and $\sigma_{\psi ij}$ are determined from respective matrices. Reaction and carryover coefficients may be calculated internally or given by input.

Next follows determination of w_{zij} (eq. (9)) pressure derivative $P_{\psi ij}$ (eq. (4)) and the pressure distribution

$$P_{ij}=P_{i1}+\int_{\psi_{\text{root}}}^{\psi} P_{\psi}\, d\psi \tag{13}$$

P_{i1} is the known root pressure at station i.

From the known pressure ratio and upstream data at station $i-1$, total velocity W_{ij} relative to blade row at station i can be determined from equation (10), and the static enthalpy h_{ij} can also be calculated. Gas specific volume is either calculated from gas law or found from computerized steam tables. An alternate simplified calculation, including the wet region, is possible using gas laws and variable specific heat ratio by numerically differentiating steam table values.

The axial velocity component, w_{ij}, derived from local velocity triangles and given Γ_{ij}/Γ_{i1} distribution, is used to force

$$r_0^2-r_{\text{root}}^2=2\int_{\psi_{\text{root}}}^{\psi_{\text{tip}}} \frac{d\psi}{k\rho w} \tag{14}$$

to approach a given value of $r_{\text{tip}}^2-r_{\text{root}}^2$ by rotating the total velocity vector W_{i1} at the root such that the modified root axial velocity is given by

$$w_{i1_{\text{mod}}}=w_{i1}\cdot\frac{r_0^2-r_{\text{root}}^2}{r_{\text{tip}}^2-r_{\text{root}}^2} \tag{15}$$

and by adjusting Γ_{i1} accordingly.

A new radius distribution,

$$r_{ij}=\sqrt{r_{i1}^2+2\int_{\psi_{\text{root}}}^{\psi_j} \frac{d\psi}{k\rho w}} \tag{16}$$

is finally calculated using a modified axial velocity,

$$w_{ij_{\text{mod}}}=w_{ij}+(w_{i1_{\text{mod}}}-w_{i1})\,\text{DC} \tag{17}$$

(DC = Damping Constant.)

Convergence is checked by comparing radii, slopes σ, and slope derivative σ_{ψ} based on the new radii with those computed in the previous iteration. Depending on these checks, the described iteration is either repeated or the system moves on to the next station. This process goes on until the downstream boundary is reached. The system will either return to the upstream boundary for a new iteration loop or move to answer calculations, depending on an overall streamline radius convergence criterion.

NUMERICAL EXAMPLES

Design Calculation

In a design case, the whole low pressure turbine is calculated in one or two sections. In the latter case an overlay is made at the joining stations in order to ensure streamline as well as thermodynamic continuity. Design information for one stage out of several calculated is shown in figures 3 through 6.

Figure 3 shows sin α (α is the nozzle exit angle) versus radial height and the partial derivative of sin α with respect to z at constant radius. The latter information allows one to account for nonradial trailing edges and other small axial adjustments during the course of design. Figure 4 relates the relative bucket entrance angle and its derivative with respect to z, and figure 5 describes the sine of the relative bucket exit angle γ and its derivative with respect to z as a function of the radius. Finally, in figure 6, the absolute stage exit angle versus radius is given. This information is the basis for the next step in designing the blade sections. Additional information such as pressure, velocity, Mach number distribution, and streamline shape is available, serving as a guide in the successive progress of a low pressure turbine layout.

Analysis of Test Conditions and Comparison of Theoretical Data with Laboratory Measurements

Calibration of the outlined procedure is of most interest. The calculation system is used for this purpose in its analysis mode to make predictions of pressure distributions, flow distributions, and flow angles at any station based on given turbine geometry, estimated efficiency, root

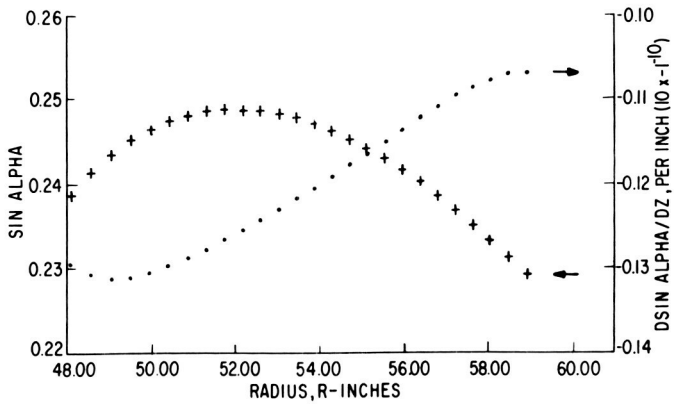

FIGURE 3.—*Design information: sine of nozzle exit angle and its derivative versus radius.*

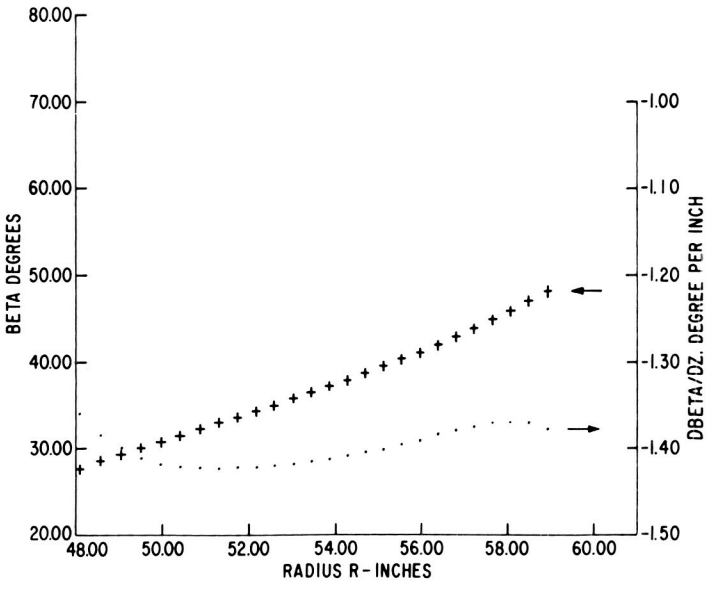

FIGURE 4.—*Design information: relative bucket entrance angle and its derivative versus radius.*

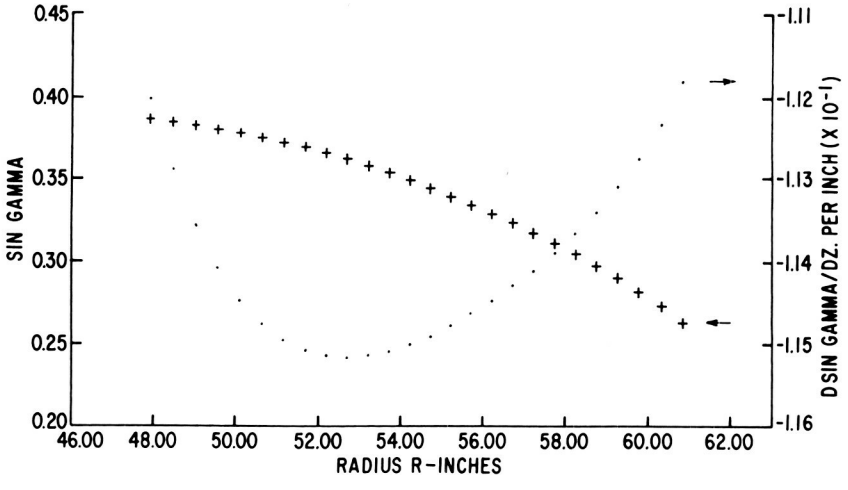

FIGURE 5.—*Design information: sine of relative bucket exit angle and its derivative versus radius.*

stage exit pressures, upstream and downstream conditions, and total flow. These predictions are compared with available traverse data behind the second, third, and fourth stage of a test turbine. Since most of the test data were accumulated under off-design conditions due to high initial

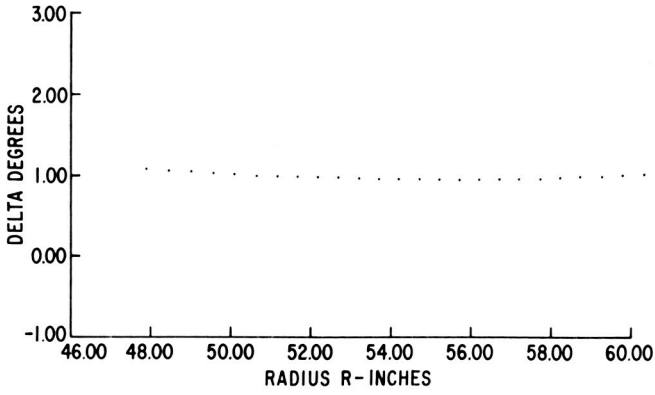

FIGURE 6.—*Design information: absolute stage leaving angle.*

superheat necessary for temperature traverses, the comparison makes for an especially good test of the capabilities of the analysis mode.

The test data presented here was obtained in the low pressure turbine test facility in the Product Development Laboratory of the Large Steam Turbine Department of General Electric Company. A detailed description of this facility is given in reference 2. The last four stages of a 30-in. low pressure turbine were tested. A cross section of the test turbine showing location of pressure taps (P), and temperature sensors (T), as well as traverse locations behind the second, third, and fourth stage is exhibited in figure 7. Figure 8 is a photo of the test rotor.

Test data (circles) and theoretical predictions (full lines) are plotted versus the respective radius ratio in figures 9 through 13.

Figures 9 and 10 present traverse data behind exit from stage number two. There is maximum discrepancy in the static pressure readings of 0.18 psia or a 2.5 percent deviation in absolute pressure level. The absolute leaving angle is negative due to lower than design velocity ratios. Calculated angles are too large, on the average by 7.8°, when the effect of tip leakage is discarded. The deviation in both graphs is in the same direction.

Comparisons of conditions at the third stage exit are shown in figures 11 and 12. The measured axial velocity decreases towards the tip less rapidly than indicated by the analysis. The leaving angle is again negative, indicating that the direction of the tangential leaving velocity is opposite to direction of wheel rotation. Calculations show angles larger on the average by 2.5°.

Average carryover and reaction coefficients were used in the calculations of the second and third stage results. In the analysis of the last stage, an estimated nozzle efficiency and the known stage streamline efficiency were used for an approximation of the bucket efficiency. The

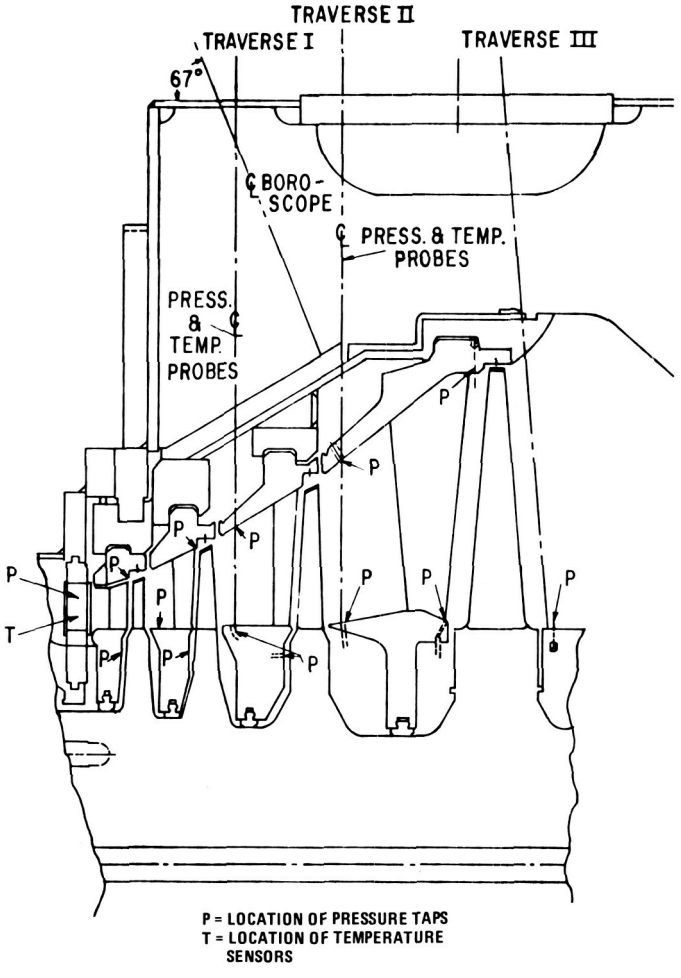

FIGURE 7.—*Cross section through test turbine.*

graph in figure 13 compares predicted and measured axial velocity distribution on a dimensionless basis.

Finally, we want to call attention to the different flow regimes that do occur in different portions of a large radius ratio low pressure steam turbine stage. The absolute velocity entering the stator is well subsonic, while the stator exit velocity ranges from supersonic at the root to subsonic at the tip as shown by the Mach number plot in figure 14. The relative exit velocities at the rotor change from transonic velocities near the root to supersonic velocities along the outer portion of the bucket. The calculation system discussed is able to analyze these stages.

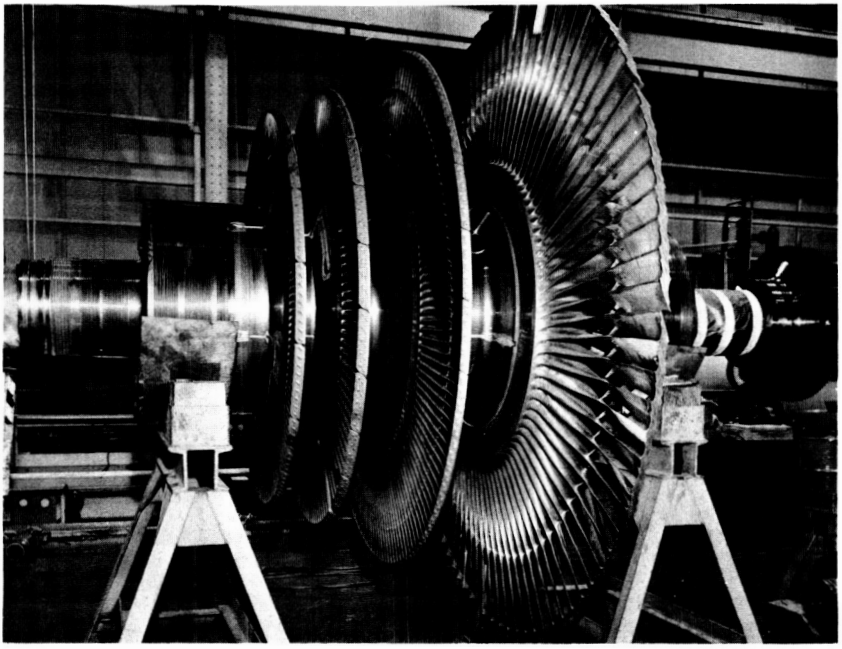

FIGURE 8.—*Thirty-inch LSB test turbine rotor.*

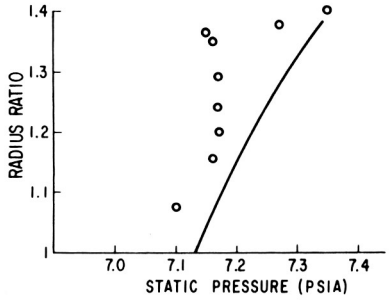

FIGURE 9.—*Comparison of predicted and measured static pressure distribution at exit of stage 2.*

FIGURE 10.—*Comparison of predicted and measured absolute leaving angle at the exit of stage 2.*

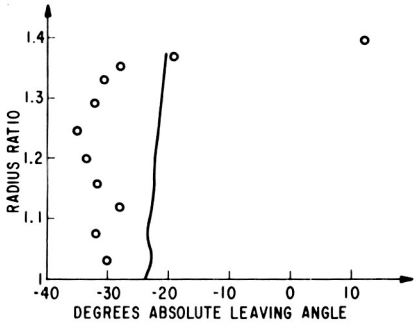

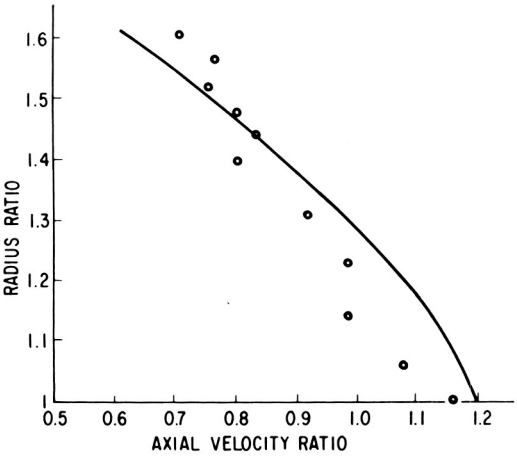

FIGURE 11.—*Comparison of predicted and measured axial velocity distribution at the exit of stage 3.*

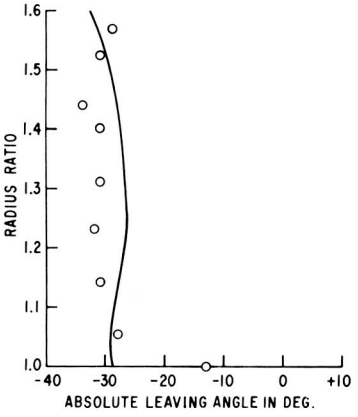

FIGURE 12.—*Comparison of predicted and measured absolute leaving angle at exit of stage 3.*

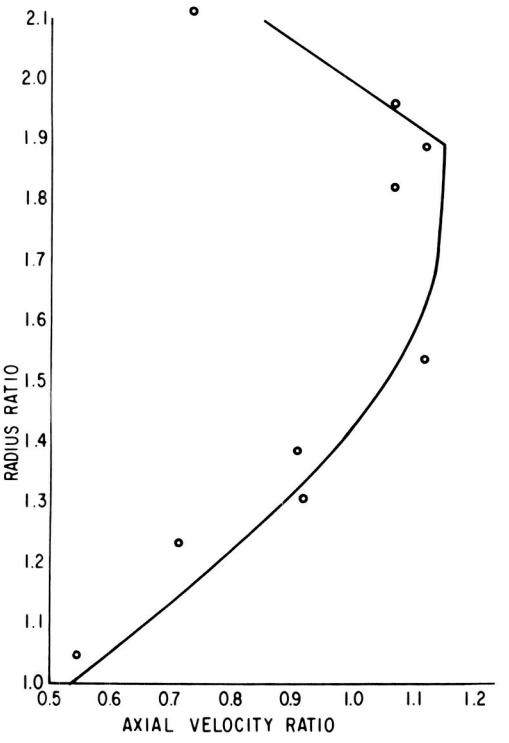

FIGURE 13.—*Comparison of predicted and measured axial velocity distribution at exit of last stage.*

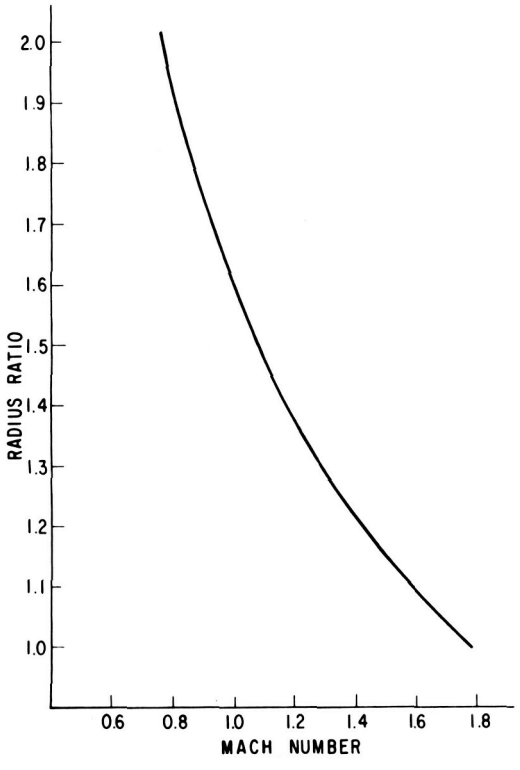

FIGURE 14.—*Mach number distribution at last stage nozzle exit.*

CONCLUSIONS

The system described has proved to be a reliable design tool. Its simple structure allows updating of the system by input of experimental data derived from tests in air and steam. The analysis mode is helpful in interpretation of test evidence. Comparison of analysis with test data shows that the system overshoots traverse data at the second stage traverse, while third and fourth stage traverses are predicted well. The match of static pressure and leaving angle depend very much on the effective nozzle areas. Differences in the axial velocity distributions can be reduced by taking account of radial bucket efficiency distribution.

REFERENCES

1. FOWLER, J. E., AND E. H. MILLER, *Some Aspects of Development of Efficient Last Stage Buckets for Steam Turbines.* ASME Paper 69–WA/Pwr–11.
2. DOWNS, J. E., AND K. C. COTTON, *Low Pressure Turbine Testing.* ASME Paper 58–SA–38.

DISCUSSION

G. K. SEROVY (Iowa State University): The author has presented a method for solution of a most difficult problem. The basic approach, as indicated by the author, is not new. It has been used to attack both design and analysis problems in axial-flow compressors, as reported independently by Smith and by Novak in ASME papers several years ago. Another closely related method was described by Renaudin and Somm of the Brown Boveri Company at a Symposium on Flow Research on Blading held in Baden, Switzerland, in 1969. The authors of earlier papers as well as this one have all succeeded in handling a very complicated situation in numerical analysis which has been encountered by all those who attempt to iterate on stream-surface shapes, especially when the flow is of a transonic character.

It would be helpful in evaluating the paper and results if the author could tell us something about the initial conditions assumed at the upstream boundary. Also he must have in his solution system some method for making an initial guess at the shapes and locations of the (ψ = constant) lines. How is this done?

In the case of axial-flow compressor calculations, it has been possible to improve solutions for the design case by using stations located inside the blade rows. It has always seemed probable to this observer that the blade-to-blade flow problem in turbines has been under control, so that such solutions (intra-blade stations) might be very feasible for steam turbines.

One might also take a certain amount of fiendish pleasure in noting that the "turbine crowd" has a most serious problem in accounting for end wall flows. We have this problem in equal or greater quantity in the "compressor crowd" and it is to be hoped that we can cooperate in developing consistent procedures for doing a better job in these regions. Mr. Herzog deserves our thanks for giving us a clear outline of his method, supported by comparison with experimental radial surveys.

H. D. LINHARDT (Airco Cryogenics): I understand the turbine you have discussed is operating under wet steam conditions in the last stage. Could you please define what are the wet steam conditions in the last stage, what is the percentage of wetness and how does the performance change when operating under wet conditions? It would be interesting to know what kind of design procedure you use and what the condensate

droplet sizes are in the last stage. How do you correlate performance and erosion phenomena with droplet size?

R. M. HEARSEY (Ohio State University Research Foundation): I wonder if you have considered modifying your procedure slightly from what I understand it to be to include the possibility of the calculation stations being nonradial, which would appear to allow you to calculate velocity distributions rather closer to the blade edges.

C. FARN (Westinghouse Research and Development): What kind of loss criteria did you use in the computation, especially for the last stage?

You only use two axial stations per stage. I always wonder whether this is accurate enough.

Is this a design program or performance program? If it's a design program, what design parameters are you specifying?

HERZOG (author): The initial conditions assumed to be given at the upstream boundary are the axial location of the station, the stagnation pressure and stagnation enthalpy, as well as the radius and slope at each streamline. Total conditions can vary from streamline to streamline.

The initial guess at shape and location of the (ψ = constant) lines is made by subdividing the flow path into a given number of equal area filaments at each station. This provides a complete radius matrix that is used to determine initial matrices for streamline slope σ_{ij} and slope derivative σ_{zij}.

Introduction of intra-blade stations is desirable and expected to improve accuracy of shape and location of the (ψ = constant) lines. As of now, we use only three stations per stage. Additional stations can be introduced into the vaneless portions of a stage. Use of nonradial stations is not planned at this time. Information needed along nonradial contours such as blade trailing edges are determined from information at the radial station which is modified by linear extrapolation either in streamline or in axial direction.

The program is mainly used as a design tool for large radius ratio steam turbines; we specify, in addition to upstream conditions, the inner and outer wall shape, blade spacing in axial direction, axial energy and reaction distribution at blade roots, and the stage total flow, wheel speed, and pressure distribution at the turbine exit. Existing components may be incorporated in new designs.

Steam entering the last stage under discussion is about $3\frac{1}{2}$ percent wet and leaves the stage at about 10 percent wet.

The performance of the turbine deteriorates with increase in initial moisture content. This effect is shown in figure D–1, which was taken from reference 2. This graph displays the change in turbine efficiency

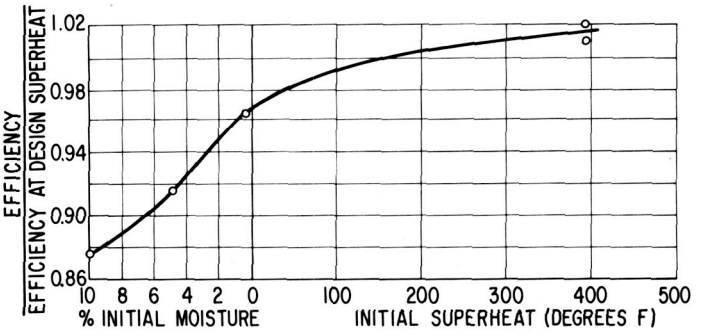

FIGURE D–1.—*Change of turbine group efficiency with change of initial steam wetness.*

with the change of the initial moisture content at the inlet of a four stage low pressure test turbine. In the range of super-heated inlet condition only part of the turbine is running on wet steam. We did not measure drop sizes in the turbine. Size measurements in a shock tunnel indicated an initial drop dimension, after spontaneous condensation took place, of submicron size. It is believed that these small drops do not cause erosion and that most of the damage is done by much larger "secondary drops" torn off the partition trailing edges. We are not aware of any laws correlating performance and erosion phenomena with drop size.